

Alignment of Perfluorinated Supramolecular Columns on the Surfaces of Various Self-Assembled Monolayers

Eun Ho Lee,[†] Dong Ki Yoon,[†] Jin Mi Jung,[†] Su Rim Lee,[†] Yun Ho Kim,[†]
Yeon-A Kim,[‡] Gunchol Kim,[‡] and Hee-Tae Jung^{*,†}

Department of Chemical and Biomolecular Engineering, Korea Advanced Institute of Science and Technology, 373-1 Guseong-dong, Yuseong-gu, Daejeon 305-701, Korea and Department of Chemistry, Chungnam National University, Gung-dong, Yuseong-gu, Daejeon 305-764, Korea

Received March 1, 2005; Revised Manuscript Received April 9, 2005

ABSTRACT: We studied the orientation of the hexagonal columnar mesophase formed by self-organization of a perfluorinated supramolecular dendrimer containing a carboxyl (–COOH) headgroup and three perfluorinated (–CF₃) tails at surfaces modified with self-assembled monolayers (SAMs). The SAM-modified surfaces studied were composed of an Au(111) substrate modified with one of five types of SAM. The SAM molecules used all had an –SH headgroup, but different terminal groups (–CF₃, –CH₃, and –OH) and different spacer chain lengths. Atomic force microscopy (AFM), transmission electron microscopy (TEM), and contact angle microscopy results revealed that the lattice parameters and structure of the perfluorinated supramolecular dendrimer are retained, but the orientation of the columns is strongly affected by the characteristics of the SAM surface. The supramolecular columns took on a planar alignment on the –CF₃ and –OH terminated SAM surfaces, but exhibited a perpendicular orientation on the –CH₃ terminated SAM surface. These variations in column alignment can be attributed to the types of molecular interactions between the terminal groups of the SAM molecules and the perfluorinated core/tails of the supramolecular columns. However, the surface morphology and orientation was not affected by changing the spacer chain length of the SAM molecules used.

Introduction

Self-assembling materials such as block copolymers and supramolecules have been proposed as candidates for the creation of novel lithographic templates because of their ability to self-aggregate into nanometer-scale building blocks.^{1,2} If such systems are to be used to create periodically patterned templates, the ability to control the orientation of the cylindrical structures formed by the materials is essential. Recently, it has been shown that the cylindrical microdomains of a block copolymer take on an orientation perpendicular to the substrate in the presence of an electric field.³ This perpendicular configuration has also been shown to form simply on account of random copolymer composition.⁴ These aligned block copolymer cylinders have various potential applications; it has been suggested, for example, that they could be used as magnetic data storage devices with predicted densities as high as ~1 terabit per square inch.⁵ However, a lack of control over the orientation of the microdomains in these supramolecular cylinders represents a significant impediment to realizing ultrahigh-density arrays, although smaller feature sizes can be achieved using supramolecular cylinders than using block copolymers. The orientation of supramolecular hexagonal phases can be controlled by approaches different from those used for block copolymers because supramolecules are united by noncovalent forces that vary depending on the size and functionalities of the molecule. Previous studies on supramolecular assembly and surface adsorption have exploited the variety and high density of chemical functionalities on the periphery of dendritic molecules.

It is well-established that the thermal stability and ordering of supramolecular amphiphiles can be enhanced by incorporating semifluorinated alkyl tails because stronger intermolecular interactions enhance microsegregation of perfluorinated and perhydrogenated parts of tapered groups because of fluorophobic effects. Moreover, the stability of perfluorinated supramolecules could potentially be further enhanced by increasing their conformational rigidity.^{6–8}

Here we present the first report on the orientation of perfluorinated supramolecular cylinders when adsorbed to solid substrates modified using various self-assembled monolayer (SAM) materials. SAMs are highly ordered molecular assemblies that chemisorb onto the surfaces of appropriate solid substrates. SAMs have the advantages that they are easy to fabricate, can be produced with a high degree of perfection, have good chemical stability under ambient conditions, and have flexibility in regard to chemical and therefore surface functionalities. Moreover, the stable and dense molecular-scale packing of SAMs, as well as the ability to control their chemical functionalities, means that SAM surfaces can be produced that are atomically flat and impenetrable. In addition, SAM-covered substrates can be modified by conventional photolithography or advanced lithography to generate patterned surfaces.⁹ Here, we show that the characteristics of the SAM terminal groups significantly affect the orientation of the perfluorinated supramolecular columns interacting with the SAM. The synthesis and characterization of the SAMs and perfluorinated supramolecular columns are also described.

Experimental Section

Materials. The fan-shaped supramolecule used in this study (Figure 1a), which contains a carboxylic core and perfluorinated tails, was synthesized as described previously.¹⁰ The compound was prepared by basic hydrolysis of methyl

* Author to whom correspondence should be addressed.
E-mail: heetae@kaist.ac.kr. Telephone: +82-42-869-3931.
Fax: +82-42-869-3910.

[†] Korea Advanced Institute of Science and Technology.

[‡] Chungnam National University.

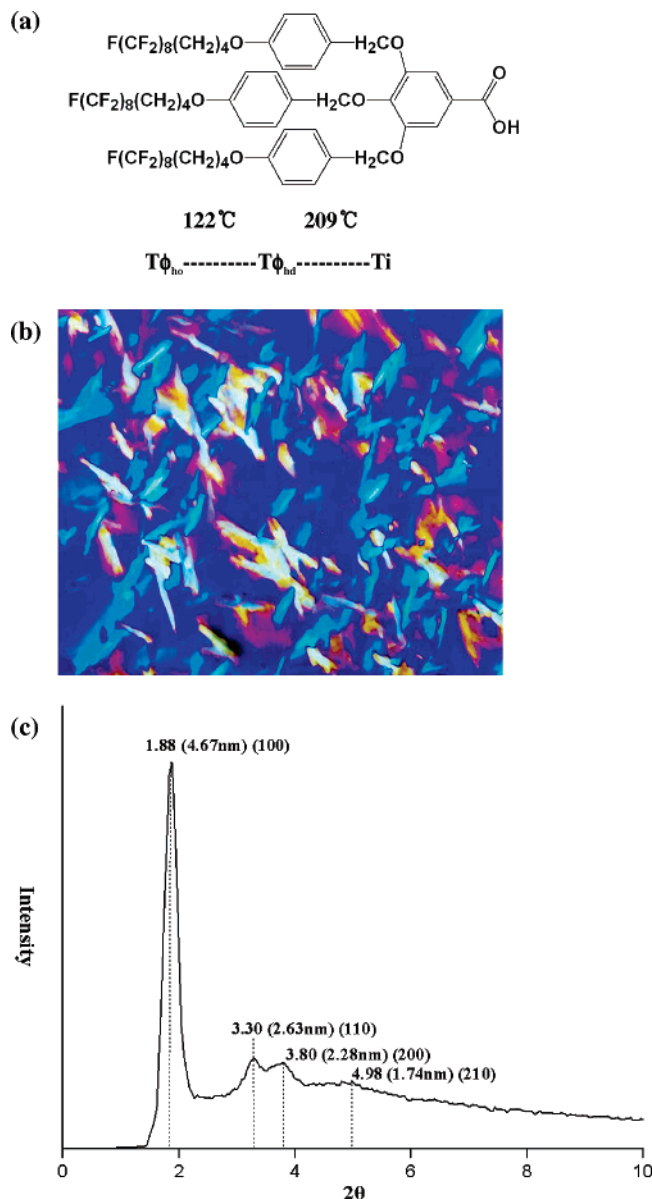


Figure 1. (a) Chemical structure of the taper-shaped dendrimer used in this study; (b) POM image of the supramolecule at $30^\circ C$; (c) X-ray diffraction pattern of the taper-shaped dendrimer at $25^\circ C$. $T_{\phi_{ho}}$, $T_{\phi_{hd}}$ and T_i represent the high-ordered hexagonal columnar, low-ordered hexagonal columnar, and isotropic transition temperatures, respectively.

3,4,5-tris[*p*-(*n*-5,5,6,6,7,7,8,8,9,9,10,10,11,11,12,12,12-hepta-decafluorododecan-1-yloxy)benzyloxy] benzoate with KOH in a mixture of ethanol and THF for 2 h under reflux, followed by acidification with 35% HCl in THF [v/v], after which the product was purified by filtration and recrystallization from acetone.

Five SAM materials were used, which we denote as SAM1 to SAM5. These materials have the same headgroup ($-SH$) but differing surface terminal tail groups ($-CF_3$, $-OH$, and $-CH_3$) and chain lengths (Figure 2). These end functionalities of the SAM materials were chosen because the supramolecule contained a hydrophilic core and perfluorinated tails. SAM1 and SAM2 have a strongly hydrophobic terminal group ($-CF_3$) but different chain lengths (SAM1, 17 carbon atoms; SAM2, 14 carbon atoms). SAM3 and SAM4 have the same hydrophilic terminal group ($-OH$), but different chain lengths (SAM3, 15 carbon atoms; SAM4, 13 carbon atoms). SAM5 is composed of a relatively neutral terminal group ($-CH_3$) and has a chain length of 12 carbon atoms. The synthetic procedures for the SAMs are given in Scheme 1.

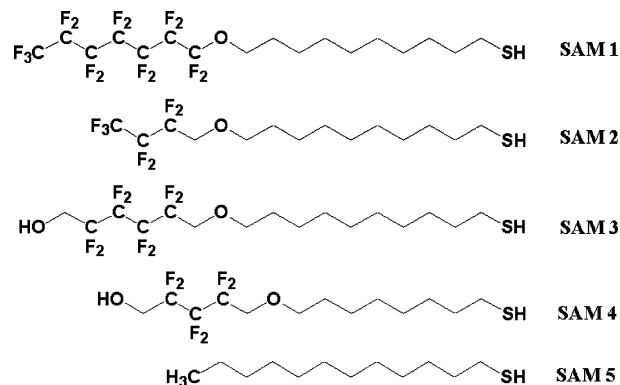


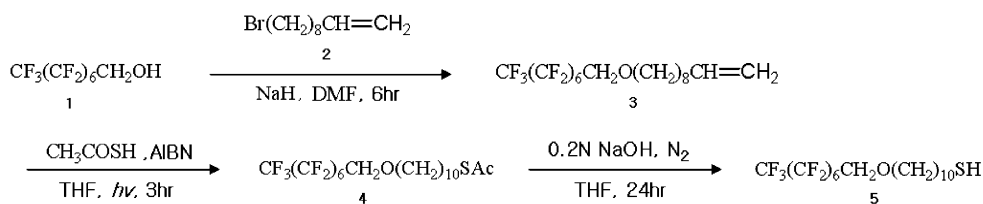
Figure 2. The five SAM molecules used in this study.

(a) Synthesis of 10-(2,2,3,3,4,4,5,5,6,6,7,7,8,8,8-penta-decafluorooctyloxy)-decane-firstiol ($C_{18}F_{15}H_{22}OSH$; SAM1). 2,2,3,3,4,4,5,5,6,6,7,7,8,8,8-pentadecafluoro-1-octanol (**1**) (98%), 10-bromo-1-decene (**2**) (97%), sodium hydride (95%), thiolacetic acid (96%), 2,2'-azobisisobutyronitrile (AIBN) (98%), and 2,2,3,3,4,4-hexadecafluoro-1,5-pentanediol (**6**) (98%) (all from Aldrich) were used as received. THF (Junsei) was dried over sodium/benzophenone and distilled freshly before use. DMF (99.9%) (Aldrich) was used as received. The purity of SAM materials was determined by thin-layer chromatography (TLC) on silica gel 60 F254 plates (Merck) with UV light (254 nm, 365 nm), where the silica gel (Grade 60, 230–400 mesh) (Merck) was used as received. The synthetic route to the novel compounds, 10-(2,2,3,3,4,4,5,5,6,6,7,7,8,8,8-pentadecafluorooctyloxy)-decane-firstiol (**5**, SAM1) is described in Scheme 1. Briefly, 10-(2,2,3,3,4,4,5,5,6,6,7,7,8,8,8-pentadecafluorooctyloxy)-1-cene (**3**) was synthesized by etherification of **2** with **1**. Compound **2** ($218\ \mu\text{L}$, $0.10\ \text{mmol}$) and NaH ($60\ \text{mg}$, $0.10\ \text{mmol}$) were combined in 3 mL of DMF under a N_2 atmosphere, and then **1** ($480\ \text{mg}$, $0.12\ \text{mmol}$) was added. After 6 h, aqueous NH_4Cl solution was added into the reaction mixture, and the mixture was extracted with CH_2Cl_2 several times, dried over $MgSO_4$, filtered, and concentrated. Thiolacetic acid ($212\ \mu\text{L}$, $2.97\ \text{mmol}$) was added into **3** ($80\ \text{mg}$, $1.49\ \text{mmol}$) and AIBN ($11\ \text{mg}$, $0.07\ \text{mmol}$) in 3 mL of THF. The resulting mixture was then exposed to UV (350 nm) radiation for 3 h, after which aqueous sodium bicarbonate solution was added and the resulting mixture was washed with CH_2Cl_2 , dried over $MgSO_4$, filtered, and concentrated by rotary evaporator, affording compound **4**. NaOH solution ($0.2\ \text{N}$) was added into **4** ($80\ \text{mg}$, $0.11\ \text{mmol}$) in 3 mL of THF. After 24 h, the resulting solution was added into water, and the reaction mixture was washed by CH_2Cl_2 , dried over $MgSO_4$, and filtered. The solvent was removed on a rotary evaporator, and SAM1 was obtained as a white powder ($56\ \text{mg}$, 74%) after purification by column chromatography (SiO_2 ; 20:1 *n*-hexane/ethyl acetate). TLC (20:1 *n*-hexane/ethyl acetate), $R_f = 0.61$. 1H NMR ($CDCl_3$, TMS, δ , ppm): 1.21 (m, 12H), 1.55 (m, 4H), 2.68 (t, 2H, $J = 7.2\ \text{Hz}$), 3.58 (t, 2H, $J = 6.4\ \text{Hz}$), 3.91 (t, 2H, $J = 14\ \text{Hz}$).

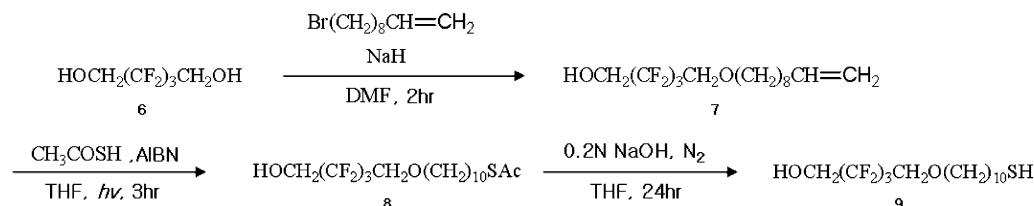
(b) Synthesis of 2,2,3,3,4,4-hexafluoro-5-(10-mercapto-decyloxy)pentan-1-ol ($C_{15}F_6H_{25}O_2SH$; SAM3). 2,2,3,3,4,4-hexafluoro-5-(9-decenyloxy)pentan-1-ol (**7**) was synthesized by etherification of **2** with **6**. Compound **2** ($190\ \mu\text{L}$, $0.94\ \text{mmol}$) and NaH ($38\ \text{mg}$, $0.94\ \text{mmol}$) were combined in 3 mL of DMF under a N_2 atmosphere, and then **6** ($200\ \text{mg}$, $0.94\ \text{mmol}$) was added. After 2 h, a saturated NH_4Cl solution was added into the reaction mixture, and the resulting mixture was extracted with CH_2Cl_2 three times. The acquired compound was dried over $MgSO_4$, filtered, and concentrated. Thiolacetic acid ($62\ \mu\text{L}$, $0.87\ \text{mmol}$) was added into **7** ($152\ \text{mg}$, $0.43\ \text{mmol}$) and AIBN ($4\ \text{mg}$, $0.02\ \text{mmol}$) in 3 mL of THF. After exposing the mixture to UV light (254 nm, 365 nm) for 3 h, a sodium bicarbonate solution was added and the resulting mixture was washed with CH_2Cl_2 , dried over $MgSO_4$, and filtered. Removal of the solvent by rotary evaporator afforded **8** ($158\ \text{mg}$, 85%).

Scheme 1. Synthesis Methods for Two Molecules for SAM Materials

1) Synthesis of 10-(2,2,3,3,4,4,5,5,6,6,7,7,8,8,8-Pentadecafluorooctyloxy)-decane-1thiol (SAM 1)



2) Synthesis of 2,2,3,3,4,4-Hexafluoro-5-(10-mercaptodecyloxy)pentan-1-ol (SAM 4)



A NaOH solution (0.2 N) was added to **8** (100 mg, 0.23 mmol) in 3 mL of THF. After 24 h, the resulting solution was added into water, and the reaction mixture was washed with CH_2Cl_2 three times, dried over MgSO_4 , and filtered. Removal of the solvent by rotary evaporator followed by purification by column chromatography (SiO_2 ; 3:1 *n*-hexane:ethyl acetate) afforded SAM3 as a white powder (90 mg, 99.8%). TLC (3:1 *n*-hexane/ethyl acetate), $R_f = 0.09$. ^1H NMR (CDCl_3 , TMS, δ , ppm): 1.21 (m, 12H), 1.55 (m, 4H), 2.23 (br s, 1H), 2.68 (t, 2H, $J = 7.2$ Hz), 3.59 (t, 2H, $J = 6.6$ Hz), 3.90 (t, 2H, $J = 14$ Hz), 4.06 (t, 2H, $J = 14$ Hz). Similar synthetic procedures were used to prepare SAM2 and SAM4. SAM5 (1-dodecanethiol) was obtained from Aldrich with 98+% purity and was used as received.

Characterization. ^1H NMR (400M Hz) spectra were recorded on a JEOL FT-NMR spectrometer. Synchrotron X-ray diffraction (XRD) measurements were conducted at 4C1 and 4C2 X-ray beam lines of the PLS synchrotron radiation source (beam energy: 5.5 keV, Pohang, Korea). The beam size at the sample was <1 mm 2 . A position-sensitive two-dimensional CCD detector was used. The sample-to-detector distance was 1000 mm, which allowed small-angle X-ray scattering (SAXS) data to be recorded. The X-ray wavelength was $\lambda = 1.5417$ Å. The SAXS data were plotted as relative intensity vs q . Heating and cooling measurements were conducted using a hot stage (Mettler FP82HT) at rates of 5 °C/min. The hydrophilic and hydrophobic modification of the substrate anchored by the SAM compound was observed by contact angle measurements using a Phoenix 300 goniometer (Surface Electro Optics Co., Ltd., Korea).

The surface topological measurements were performed under ambient conditions using AFM (SPA 400 microscope, Seiko Instruments). The silicon cantilevers of an SI-DF20S (dynamic force mode) were used for the condensed phase. The thin films were also examined at 120 kV using a Philips CM-20 TEM. Bright field phase contrast TEM images and electron diffraction (ED) patterns were obtained by low dose procedures.¹¹ For TEM specimens, a thin layer of carbon was evaporated onto the supramolecules on the treated substrates, and this carbon layer was then covered with a 25% aqueous solution of poly(acrylic acid) (PAA). After drying in air, the layer comprised of the PAA, carbon, and supramolecule films was peeled off from the SAM-treated surface by immersing the substrate in liquid nitrogen. The removed layer was then floated on deionized water with the PAA side down. When the PAA layer had completely dissolved, the floating films were collected onto a copper grid. The thin films of supramolecules on the SAM-treated substrates were cast from a solution of 1 wt % in THF onto distilled water. These thin films of thickness ~ 50 nm were annealed at 45 °C for 2 h. To improve the mass contrast and radiation sensitivity, the thin films were exposed to RuO_4 vapor (solutions of 0.5 wt % aqueous RuO_4) for 3 min.¹²

Results and Discussion

Synchrotron X-ray diffraction (XRD), DSC (not shown here) and polarized optical microscopy (POM) results (Figure 1) show that the supramolecule used in the present study (Figure 1a) forms dendrimers exhibiting a hexagonal columnar mesophase upon cooling from the isotropic phase. Upon cooling at a rate of 5 °C/min, the dendrimer exhibits a low-ordered hexagonal mesophase transition at 209 °C from the isotropic melt, followed by a high-ordered hexagonal columnar phase transition at 121.8 °C. A POM image recorded at room temperature (Figure 1b) shows that the material exhibits a fan-shaped focal conic texture, which is one of the characteristic textures of a columnar mesophase. The XRD spectrum (Figure 1c) shows narrow reflections at small angles but broad bands centered at ~ 0.5 nm. This indicates that the molecules are arranged in periodic structures, but with a disordered structure at the atomic level. The relative positions of the scattering peaks of the supramolecule are 1, $\sqrt{3}$, 2, and $\sqrt{7}$, which are consistent with hexagonal packing with an average diameter of 5.39 nm.

SAMs of five types of molecules (Figure 2) were deposited on a Au(111) surface. All five molecules (SAM1–5) had a thiol headgroup that interacts with gold. The Au substrate was prepared by depositing a highly uniform layer of gold (~ 200 nm thick) onto a Si(111) wafer by E-beam evaporation. The Au surface was cleaned by immersion in freshly prepared piranha solution (sulfuric acid/hydroperoxide (3:1)) for 1 min followed by several rinsings with ethanol and deionized water. The SAM was deposited on the Au(111) surface by immersing the Au substrate into a 1 mM solution of the SAM compound for at least 20 h to ensure good coverage.¹³ Dichloromethane was used as the solvent for SAM1–4, whereas ethanol was used for SAM5. The treated substrates were washed with ethanol to remove the molecules beyond the monolayer. Although the mechanistic details of this reaction remain incompletely understood, the thiol group is readily chemisorbed onto gold. It is generally believed that the thiol group forms a thiolate in its interaction with gold.^{14–16}

Figure 3a and b show high-resolution nonfiltered AFM images and their corresponding Fourier transform power spectra (inset) of the supramolecular columns on the surfaces covered with SAM1 (containing a perfluorinated ($-\text{CF}_3$) terminal group) and SAM3 ($-\text{OH}$

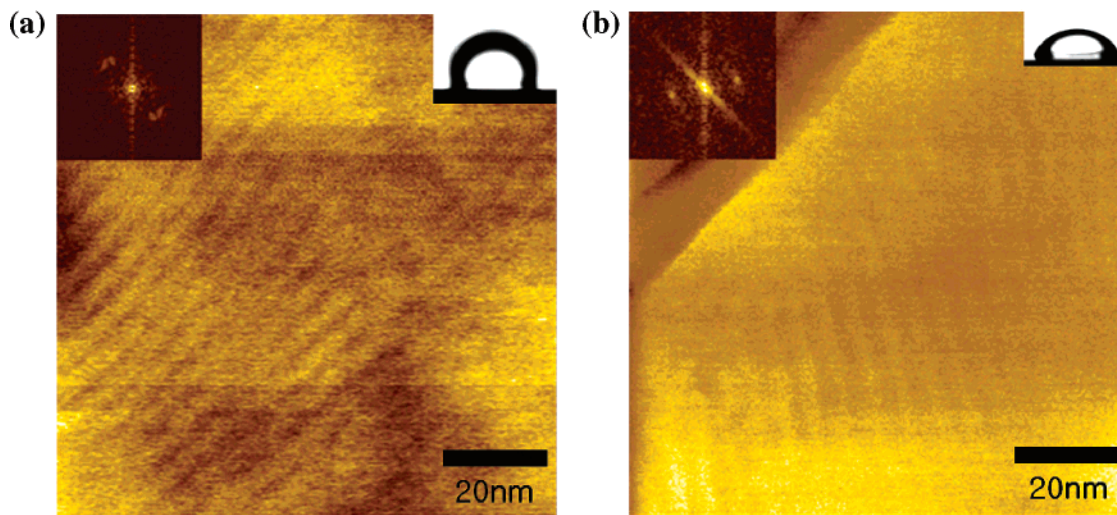


Figure 3. AFM micrograph showing the planar orientation of hexagonal cylinders on SAMs; (a) A $100 \times 100 \text{ nm}^2$ AFM image on SAM1; (b) A $100 \times 100 \text{ nm}^2$ AFM image on SAM4.

terminal group), respectively. A planar alignment was obtained in both cases. The cylinders are coherently aligned and are elongated along the cylinder axis. The (10) spacing of the columns on the SAM1 surface was estimated to be $\sim 4.7 \text{ nm}$ from the power spectrum. This spacing is consistent with the XRD measurement (Figure 1c), indicating that the microstructure of the supramolecular columns is retained on the SAM1 surface. Identical results were obtained for the SAM2 surface, confirming that the space chain length of the SAMs does not affect the structure and orientation of the supramolecular columns.

Planar alignment was also obtained on the surfaces of the monolayers of SAM3 and SAM4, both of which contain a $-\text{OH}$ terminal group (Figure 3b). This result is unexpected because SAM3 and SAM4 show significantly different interfacial properties such as wetting and adhesion properties (see insets of Figure 3, contact angle images). As for the SAM1 and SAM2 systems, the lattice parameter was the same for SAM3 and SAM4, regardless of their different space chain lengths.

The very different surface properties of $-\text{CF}_3$ -terminated SAMs and $-\text{OH}$ -terminated SAMs suggest that the planar alignment observed for both of these surface types may arise via different mechanisms. Thus, the tendency to form a planar alignment can be understood in terms of the molecular interactions between the terminal groups of the SAMs and the perfluorinated core/tails of the supramolecular columns because the self-assembly behavior of the dendrimer strongly depends on the wedge shape of the molecules and the strength of the inter- and intramolecular interactions. Given that the supramolecule used in this study is composed of a hydrophilic carboxylic core group ($-\text{COOH}$) and strong hydrophobic perfluorinated tails, they may be oriented differently depending on the interactions between the core and tails of the supramolecule and the chemical functionality of the SAM adhered to the Au substrate. Consistent with these pictures, the contact angles of the SAMs comprised of SAM1, SAM4, and SAM5 were 109° , 86° , and 52° , respectively (see insets of Figures 3 and 4). The processes that give rise to these different contact angles are depicted schematically in Figure 5.

At the surfaces covered with $-\text{CF}_3$ -terminated SAMs (SAM1 and SAM2), the peripheral $-\text{CF}_3$ tail groups of

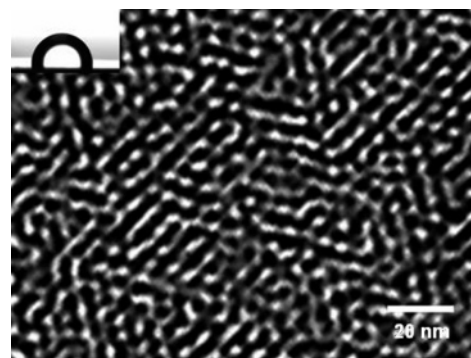


Figure 4. TEM micrograph of homeotropically aligned hexagonal cylinders on SAM5.

the supramolecule, which make the dendrimer strongly hydrophobic, are likely in direct contact with the SAM1 and SAM2 surfaces because of the strong chemical affinity between the $-\text{CF}_3$ on the supramolecule tails and the $-\text{CF}_3$ terminal group on the SAMs (Figure 5a). Moreover, the dendrimer is highly microphase-separated around the center of the core group, and each single slice of the columns may be strongly associated with other such slices.^{13,17} As a result, the core groups are oriented away from the substrate. The cylinders ultimately self-organize into a planar alignment, as confirmed by AFM (Figure 3a).

In the case of the planar alignment on SAM3 and SAM4, the carboxyl core ($-\text{COOH}$) of the dendrimer turns toward the hydroxyl ($-\text{OH}$) surface groups of the SAM to maximize the strong hydrophilic interactions that occur in this configuration (Figure 5b). This causes the hydrophobic $-\text{CF}_3$ tail groups of the dendrimer to be oriented away from the hydrophilic substrate. In other words, a dense monolayer of wedge-shaped molecules, which may consist of fractional columns, forms on the $-\text{OH}$ -terminated surface. Additional characteristics of the multilayer structure, as described above, depend on the wedge shape of the supramolecules and the microphase separation caused by the different affinity between the hydrophilic core and strong hydrophobic tails.

At the surface covered with the $-\text{CH}_3$ -terminated SAM5, the columns of supramolecules are aligned

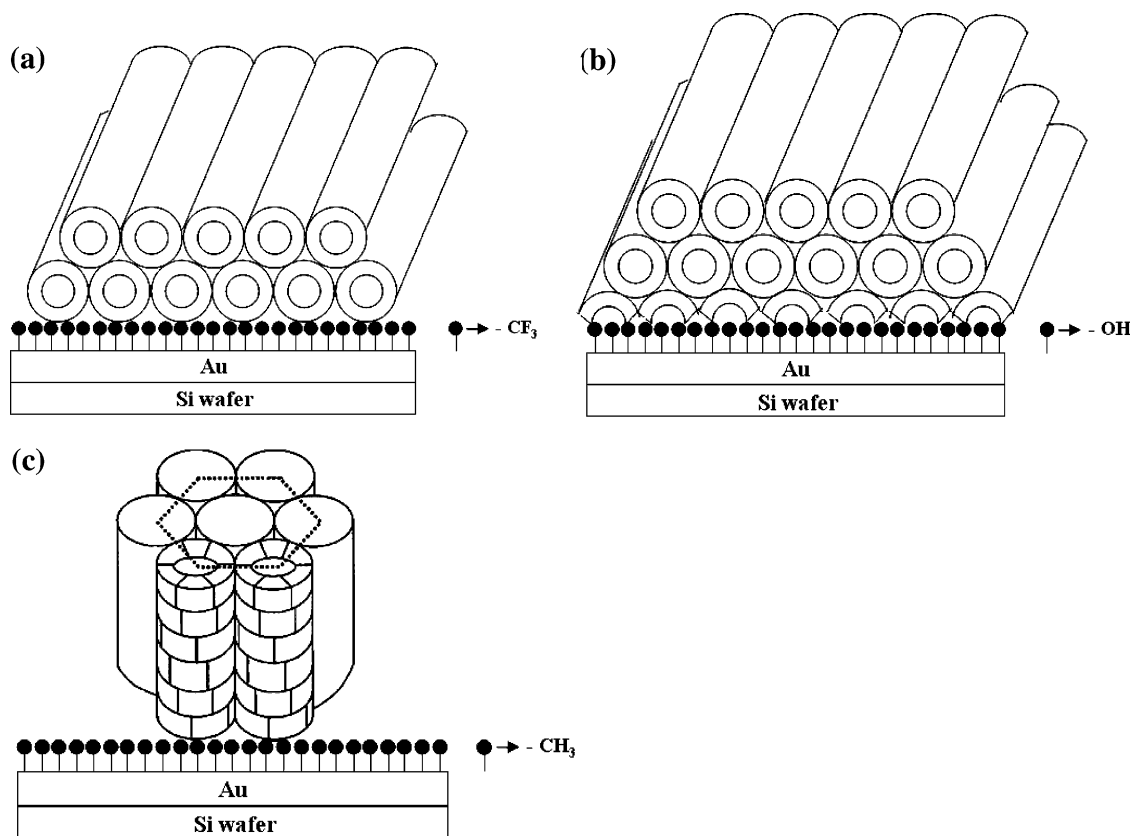


Figure 5. Schematic representation of (a) planar-aligned ϕ_h LC assembly generated by tapered amphiphilic supramolecular columns on SAM1 and SAM2; (b) planar-aligned ϕ_h on SAM3 and SAM4; and (c) homeotropically aligned ϕ_h on SAM5.

normal to the surface (Figure 4). On the basis of AFM observations, it was impossible to verify whether the columns were vertically aligned on the surfaces just because there is no difference in the columns' height. The cylindrical moieties on this surface are packed into a highly ordered hexagonal lattice configuration showing 6-fold symmetry. In the TEM image, the cylinder cores appear dark. Given that RuO_4 vapor selectively stains the aromatic and ether portions of molecules, we can conclude that these portions of the supramolecules lie at the cores of the cylinders, consistent with the expected molecular orientation. This configuration may be preferred on relatively noninteracting neutral substrates because it accommodates the flat-equilibrium molecular conformation, or face-on configuration, as described in other studies.^{18,19} The alkyl group may not interact strongly with either the core or the tails of the supramolecules. In addition, the supramolecule contains flat aromatic molecules, which may interact with the alkyl-terminated SAM5 surface. Moreover, the perpendicular orientation of the fan-shaped supramolecules is energetically favored over the planar orientation (Figure 5c).

Conclusions

The present study of the self-organization of a perfluorinated supramolecule against a substrate covered with a SAM shows that the orientation of the hexagonal columnar mesophase formed by self-organization of the perfluorinated supramolecule is sensitive to the characteristics of the SAM molecules. In particular, SAMs comprised of molecules containing a thiol group on one end and the functional group, $-\text{CF}_3$, $-\text{CH}_3$, or $-\text{OH}$, on the other end were effective for controlling the

orientation of the supramolecular cylinders because the perfluorinated supramolecular dendrimers contain carboxyl groups in the core of the cylinder and perfluorinated tails.

On the $-\text{CF}_3$ - and $-\text{OH}$ -terminated SAM surfaces, supramolecular columns were organized in a planar alignment. On the $-\text{CH}_3$ -terminated SAM surface, by contrast, a perpendicular column orientation was favored. The tendency to form a planar alignment at the $-\text{CF}_3$ -terminated SAM surfaces can be attributed to strong molecular interactions between the CF_3 group of the SAM and the perfluorinated tails of the supramolecular columns. In contrast, the planar alignment observed on the $-\text{OH}$ -terminated SAM surfaces can be attributed to the interaction between the carboxyl cores ($-\text{COOH}$) of the supramolecular columns and $-\text{OH}$ groups of the SAM molecules. The tendency to form homeotropic cylinders on the $-\text{CH}_3$ -terminated SAM surface results from the noninteracting neutral surface and the molecular shape of the perfluorinated supramolecule. The present results on the orientation of supramolecular cylinders should prove useful in practical applications because the SAMs of alkanethiolates on gold studied here can serve as models or prototypes for new techniques or applications that will be generally applicable to new classes of SAMs designed specifically for microprocessing and microfabrication.

Acknowledgment. This work was supported by Korea Research Foundation Grant (KRF-2003-041-D20190) and the Brain Korea 21 Program. We thank the Pohang Accelerator Laboratory for providing the 4C1 and 4C2 beam-lines used in this study.

References and Notes

- (1) Clark, T. D.; Ferrigno, R.; Tien, J.; Paul, K. E.; Whitesides, G. M. *J. Am. Chem. Soc.* **2002**, *124*, 5419.
- (2) Hudson, S. D.; Jung, H.-T.; Percec, V.; Cho, W.-D.; Johansson, G.; Ungar, G.; Balagurusamy, V. S. K. *Science* **1997**, *278*, 449.
- (3) Mansky, P.; DeRouchey, J.; Russell, T. P.; Mays, J.; Pitsikalis, M.; Morkved, T.; Jaeger, H. *Macromolecules*, **1998**, *31*, 4399.
- (4) Morkved, T. L.; Lu, M.; Urbas, A. M.; Ehrichs, E. E.; Jaeger, H. M.; Mansky, P.; Russell, T. P. *Science*, **1996**, *273*, 931.
- (5) Kim, H.-C.; Jia, X.; Stafford, C. M.; Kim, D. H.; McCarthy, T. J.; Tuominen, M.; Hawker, C. J.; Russell, T. P. *Adv. Mater.* **2001**, *13*, 795.
- (6) Smart, B. E.; Banks, R. E.; Tatlow, J. X. In *Organofluorine Chemistry: Principles and Commercial Applications*; Banks, R. E., Smart, R. E., Tatlow, J. C., Eds.; Plenum: New York, 1994; p 57.
- (7) Eaton, D. F.; Smart, B. E., *J. Am. Chem. Soc.*, **1990**, *112*, 2821.
- (8) Percec, V.; Schlueter, D.; Ungar, G.; Cheng, S. Z. D.; Zhang, A. *Macromolecules* **1998**, *31*, 1745.
- (9) Hong, L.; Sugimura, H.; Furukawa, T.; Takai, O. *Langmuir* **2003**, *19*, 1966.
- (10) Percec, V.; Johansson, G.; Ungar, G.; Zhou, J. *J. Am. Chem. Soc.* **1996**, *118*, 9855.
- (11) Jung, H.-T.; Hudson, S. D.; Lenz, R. W. *Macromolecules* **1998**, *31*, 637.
- (12) Jung, H.-T.; Kim, S. O.; Hudson, S. D.; Percec, V. *Appl. Phys. Lett.* **2002**, *80*, 395.
- (13) Johansson, G.; Percec, V.; Ungar, G.; Zhou, J. P. *Macromolecules* **1996**, *29*, 646.
- (14) DiMilla, P.; Folkers, J. P.; Biebuyck, H. A.; Harter, R.; Lopez, G.; Whitesides, G. M. *J. Am. Chem. Soc.* **1994**, *116*, 2225.
- (15) Alves, C. A.; Porter, M. D. *Langmuir* **1993**, *9*, 3507.
- (16) Poole, C. P.; Owens, F. J. *Introduction to Nanotechnology*; Wiley-Interscience: New York, 2003; p 260.
- (17) Percec, V.; Cho, W.-D.; Ungar, G. *J. Am. Chem. Soc.* **2000**, *122*, 10273.
- (18) Mindyuk, O. Y.; Heiney, P. A. *Adv. Mater.* **1999**, *11*, 341.
- (19) Pao, W.-J.; Stetzer, M. K. R.; Heiney, P. A.; Cho, W.-D.; Percec, V. *J. Phys. Chem. B* **2001**, *105*, 2170.

MA050427W